Coseismic off-fault antithetic shear deformation in southwestern Taiwan triggered by the 2016 M_w 6.4 Meinong earthquake

Ruey-Juin Rau[1], Li-Chia Lai[1], Kuo-En Ching[2]

[1]Department of Earth Sciences, National Cheng Kung University, Taiwan

[2]Department of Geomatics, National Cheng Kung University, Taiwan

EGU23-1803

1. Abstract

We used 70 campaign-mode, 12 continuous and 6 high-rate GNSS and InSAR data to examine the coseismic off-fault antithetic shear triggered by the 2016 M_w 6.4 Meinong oblique thrust earthquake at the Hsinhua fault area, ~30 km northwest of the epicenter. The GNSS and InSAR data were inverted to estimate the 3D coseismic displacement field at the Tainan frontal fold-thrust belt, where the deformation is mostly affected by the directivity along the rupture front direction of the Meinong earthquake. The coseismic deformation pattern shows dominantly synthetic shear along the rupture direction, on the contrary, a nearly N-S striking, 7-km-long and 5-km-wide area indicating antithetic motion appeared at northeast of the Tainan tableland and cross-cutting the ENE-WSW-striking Hsinhua fault at a high angle. The N-S striking structure at the Hsinhua fault area reveals coseismic horizontal displacements of 3.0-7.0 cm to the southeast and vertical displacements of 0.4 to 4.4 cm, and although in the opposite direction, the magnitude of horizontal displacements of the antithetic shear are comparable to those of the synthetic motion in the adjacent areas. We calculated the static Coulomb stress change on the possible west-dipping shallow structure at the Hsinhua area due to slip on the source fault of the 2016 Meinong earthquake. The calculated static stress change is about 0.05 bar, which is negligible and very unlikely to promote the structure or bedding to slip at 30-km away for such a moderate earthquake. We also processed 6 high-rate, two 50-Hz and four 1-Hz, GNSS data for the PPP displacement and SNIVEL GPS-derived velocities, in that two stations, one 50-Hz and one 1-Hz, are located inside the block with antithetic motion. The high-rate GNSS solutions indicate that the displacements occurred at the same time when the P and S waves arrived, and velocity pulses up to 90.0 cm/s appeared at all six stations. We suggest that, as evidenced by large velocity pulses resulted from the strong directivity effect, the dynamic stress change caused by the rupture of the 2016 Meinong earthquake triggered the structure 30-km away.

2. Antithetic deformation in SW Taiwan during 2016 Mw 6.4 Meinong earthquake

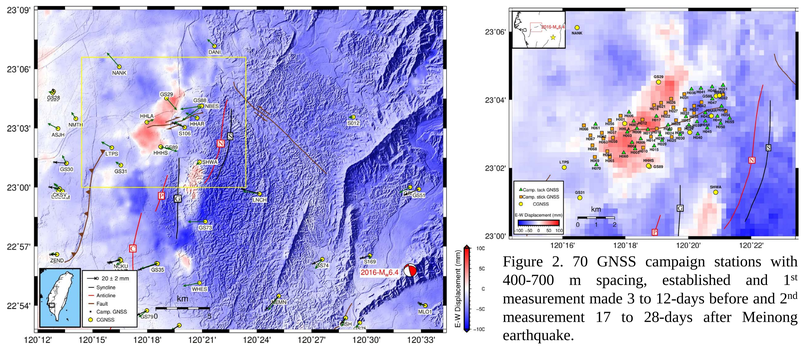

Figure 1. Coseismic InSAR-derived E-W (modified from Huang et al., 2016) and GNSS displacements during 2016 Meinong earthquake. Yellow circles are the GNSS stations. Black dots are the campaign GNSS stations. Black and green arrows are GNSS coseismic displacements from Huang et al. (2016) and this study, respectively.

Figure 2. 70 GNSS campaign stations with 400-700 m spacing, established and 1st measurement made 3 to 12-days before and 2nd measurement 17 to 28-days after Meinong earthquake.

Questions:

- **What is the structure responsible for the antithetic deformation?**
- **What is the triggering mechanism?**

3. Geology background of Tainan

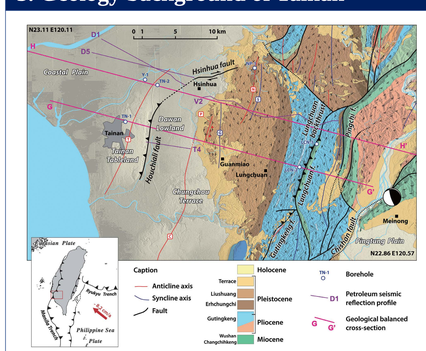

Figure 4. A conceptual geology model of the Hsinhua section. No evidence of weak bedding interface or fault in the stratigraphy of shallow structure.

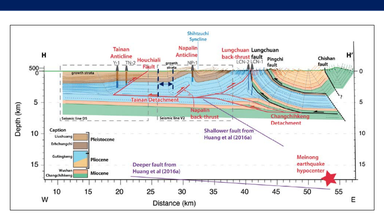

Figure 3. Left: Geology map of Tainan area (Le Béon et al., 2017). Geological cross section of HH' is shown above.

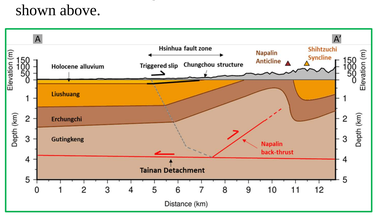

4. Continuous GNSS time series

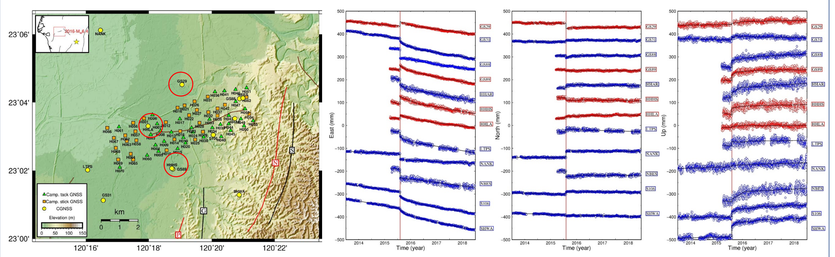

Figure 5. GNSS station map and EW, NS and Vertical displacement time series of continuous GNSS stations. Red lines are the stations of antithetic deformation.

5. Coseismic displacements at the Hsinhua area

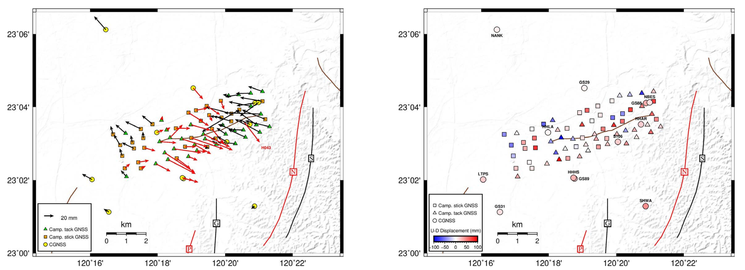

Figure 6. Coseismic GNSS displacements at the Hsinhua area. Left: horizontal, right: vertical.

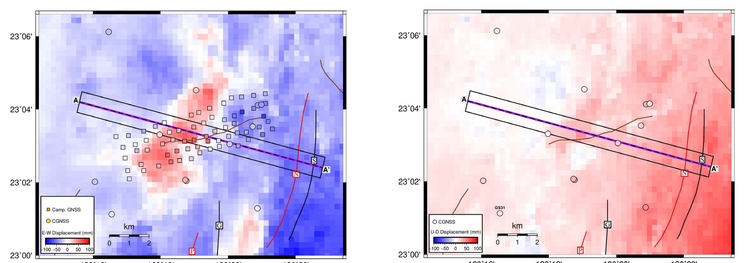

Figure 7. Coseismic GNSS overlap with InSAR (Lu et al., 2018) displacements at the Hsinhua area. Left: horizontal, right: vertical.

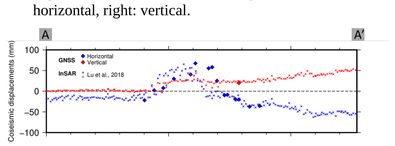

Figure 8. Cross section AA' comparison of Coseismic GNSS and InSAR displacements (Lu et al., 2018) at the Hsinhua area.

6. Coseismic antithetic deformation and local structures

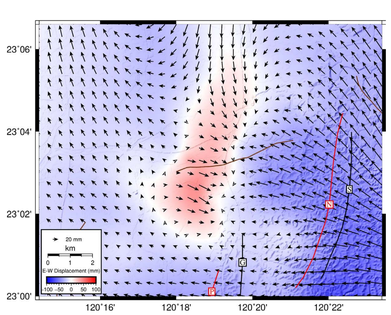

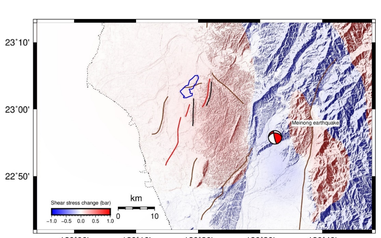

Figure 9. Left: E-W displacement resulted from velocity inversion at the Hsinhua area. Right: Calculated static stress change map.

7. High rate GNSS PPP solutions

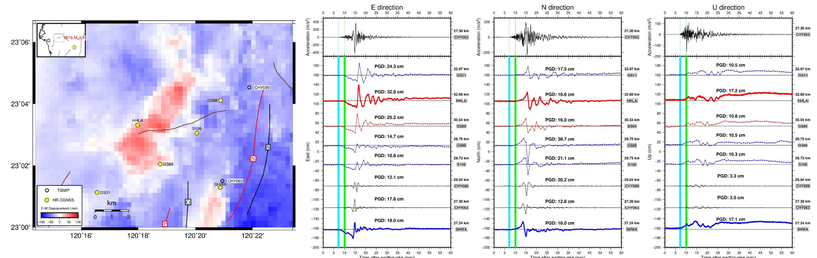

Figure 10. Left: E-W displacement and high-rate GNSS stations at the Hsinhua area. Right: Strong motion and high-rate GNSS stations displacement time series. Antithetic deformation is closely related to stations with large PGD.

8. Antithetic deformation is dynamically triggered by large velocity pulse generated by 2016 Meinong earthquake

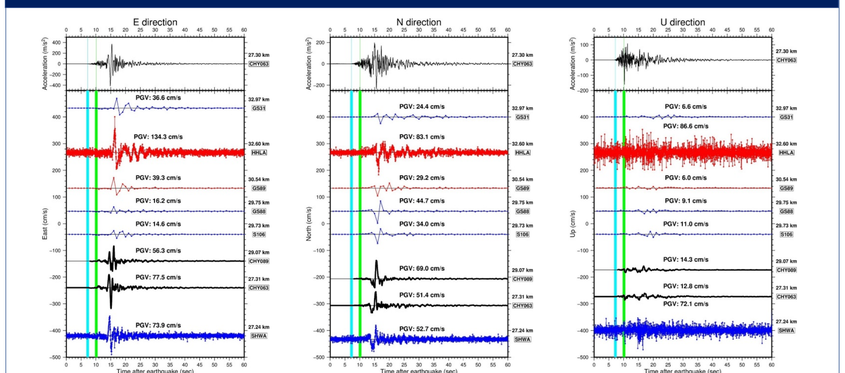

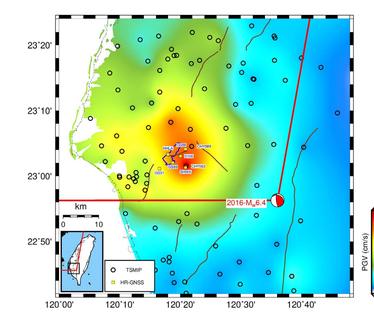

Figure 11. Upper: Strong motion and high-rate GNSS stations velocity time series. Antithetic deformation is closely related to stations with large velocity pulse. GNSS velocity solutions: SNIVEL (Crowell, 2021). Lower: PGV of 2016 Meinong earthquake.

9. Coseismic maximum principal strain field

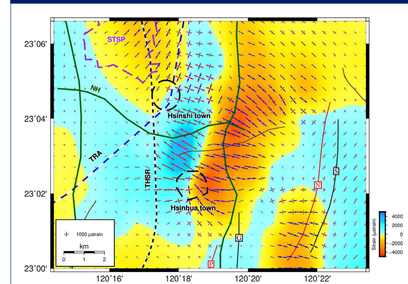

Figure 12. Coseismic maximum principal strain map of the Hsinhua area.

10. Conclusions

- Antithetic deformation is dynamically triggered by large velocity pulse generated by the 2016 Meinong earthquake.
- Antithetic deformation is unlikely resulted from reactivation of any W-dipping structures due to no evidence of weak bedding interface or fault in the stratigraphy of shallow structure in SW Taiwan.
- Reactivation of mud-diapir, which is very common in SW Taiwan, is likely the cause of antithetic deformation during Meinong earthquake, as evidenced in the coseismic strain field map.

11. References

Crowell, B. W. (2021). Near-Field Strong Ground Motions from GPS-Derived Velocities for 2020 Intermountain Western United States Earthquakes. *Seismol. Res. Lett.* 92, 840–848, doi: 10.1785/0220200325.

Lu, C. H., Ni, C. F., Chang, C. P., Yen, J. Y., & Chuang, R. Y. (2018). Coherence difference analysis of sentinel-1 SAR interferogram to identify earthquake-induced disasters in urban areas. *Remote Sens., 10*(8), 1318, doi:10.3390/rs10081318.

Le Béon, M., M. H. Huang, J. Suppe, S. T. Huang, E. Pathier, W. J. Huang, C. L. Chen, B. Fruneau, S. Baize, K. E. Ching, and J. C. Hu. (2017). Shallow geological structures triggered during the Mw 6.4 Meinong earthquake, southwestern Taiwan. *Terr. Atmos. Ocean. Sci., 28*(5), 661-681, doi: 10.3319/TAO.2017.03.20.02.

Huang, M. H., Tung, H., Fielding, E. J., Huang, H. H., Liang, C., Huang, C., & Hu, J. C. (2016). Multiple fault slip triggered above the 2016 Mw 6.4 MeiNong earthquake in Taiwan. *Geophys. Res. Lett., 43*, 7459–7467, doi:10.1002/2016GL069351.